Taylor & Francis
Taylor & Francis Group

Highly Efficient Phosphorescent Blue Organic Light-Emitting Diodes Based on Double-Emitting Layer

JUNG SUN PARK,[1] JI HOON SEO,[1] BO MIN SEO,[1]
JA RYONG KOO,[1] KUM HEE LEE,[2]
SEUNG SOO YOON,[2] AND YOUNG KWAN KIM[1]

[1]Department of Information Display, Hongik University, Seoul, Korea
[2]Department of Chemistry, Sungkyunkwan University, Suwon, Korea

In this paper, We have demonstrated lower driving voltage and efficient Blue phosphorescent organic light emitting diodes (PHOLEDs) using iridium (III) bis[(4,6-di-fluoropheny)-pyridinato-N,C²] picolinate doped in N,N'-dicarbazolyl-3,5-benzene (mCP) and 2,2',2''-(1,3,5-benzenetryl)tris(1-phenyl)-1H-benzimidazol (TPBi) as double-emitting layer system. D-EML layers were employed to have good exciton confinement. We also demonstrated that mCP as electron blocking layer inserted EML and HTL for higher efficiency. The optimized device of double EML of mCP:TPBi(1:1) exhibited a maximum external quantum efficiency of 9.22% at 0.21 mA/cm², a maximum Current efficiency of 18.89 cd/A at 0.21 mA/cm², and Commission Internationale de I'Eclairage coordinates of (0.17, 0.35) at 1000 cd/m², respectively.

Keywords Blue phosphorescent organic light emitting diodes; double-emitting layer; energy transfer; exciton confinement

Introduction

Since the first report on light emission from organic light-emitting diodes (OLEDs) by Tang and Van Slyke, advances of red, green, and blue organic materials, device structures, and manufacturing processes have led to the demonstration of full-color OLEDs [1–5]. Especially, phosphorescence OLEDs (PHOLEDs) using green and red emitting devices have reached almost 100% internal quantum efficiency by efficient utilizing both singlet and triplet excitons [6–8]. As a result, low driving voltage and high power efficiency have been achieved for phosphorescent red- and green-emitting devices. However, the performance of phosphorescent blue emitting devices still need to be improved for full-color displays and lighting applications. Therefore many researchers have studied PHOLEDs for phosphorescent blue double-emitting layer (D-EML) and higher triplet exciton blocking layer inserted between the EML

Address correspondence to Prof. Young Kwan Kim, Department of Information Display, Hongik University, Sangsu-dong, Mapo-ku, Seoul 121-791, Korea (ROK). Tel.: (+82)2-320-1646; Fax: (+82)2-3142-0335; E-mail: kimyk@hongik.ac.kr

and hole transporting layer (HTL) because of efficient charge trapping and exciton confinement for high efficiency [9–11]. Recently, Yook *et al.* [9] presented the D-EML by using iridium (III) bis[(4,6-di-fluoropheny)-pyridinato-N,C^2] picolinate (FIrpic) doped in D-EML, N,N′-dicarbazolyl-3,5-benzene (mCP) and 1,3-bis(triphe-nylsilyl)benzene (UGH3). However, the highest occupied molecular orbital (HOMO) value of UGH3 is about 7.1 eV, which may result in a larger barrier for holes injection. In this paper, we demonstrated efficient blue PHOLEDs by using FIrpic doped in D-EML, mCP and 2,2′,2″-(1,3,5-benzenetryl)tris(1-phenyl)-1H-benzimida-zol (TPBi) [12]. The optimized blue PHOLEDs showed a peak external quantum efficiency (EQE) of 9.22% at 0.21 mA/cm^2, power efficiency of 12.62 lm/W at 0.05 mA/cm^2, Current efficiency of 18.89 cd/A at 0.21 mA/cm^2, and Commission Internationale de I'Eclairage coordinates (CIE$_{x,y}$) of (0.17, 0.35) at 1,000 cd/m^2, respectively.

Experimental

Glass substrate coated with a 150-nm-thick indium tin oxide (ITO) layer has a sheet resistance of 12 Ω/sq. ITO manufactured by Sunic System was cleaned with acetone, methanol, distilled water, and isopropyl alcohol in ultrasonic bath. Then, pre-cleaned ITO was treated by O2 plasma treatment with the conditions of 2×10^{-2} Torr, 125 W, and 2 min. All organic layers were sequentially deposited onto the substrate without breaking vacuum at a pressure of about 5×10^{-7} Torr, using the thermal evaporation equipment. The deposition rates were 1.0–1.1 Å/sec for organic materials and 0.1 Å/sec for lithium quinolate (Liq), respectively. Finally, the aluminum cathode was deposited at a rate of 10 Å/sec. The doping concentra-tions of dopants were optimized. The devices were encapsulated immediately after preparation under nitrogen atmosphere. With the DC voltage bias, the electrolumi-nescence (EL) spectrum, current density, current efficiency, power efficiency and luminance characteristics were measured with a spectrora diometer of Minolta CS-1000 instrument. A digital source meter (Keithley 236) and a desktop computer used to operate the devices were connected. The EQE and CIE$_{x,y}$ coordinates were calculated. All measurements were carried out under ambient conditions at room temperature.

Results and Discussion

Figure 1(a) shows the chemical structures of the key materials used in this study, FIr-pic as phosphorescent blue emitter, mCP and TPBi as phosphorescent blue host, respectively. Figure 1(b) shows energy level diagram of blue OLED devices which have the following structure: ITO as anode/N,N′-bis-(1-naphly)-N,N′-diphenyl-1,1′-biphenyl-4,4′-diamine (NPB) as hole transporting layer (HTL)/mCP as exciton blocking layer (XBL) [13]/FIrpic doped in mCP as blue emitting layer (BEML-1)/ FIrpic doped in TPBi as blue emitting layer (BEML-2)/4,7-diphenyl-1,10-phenanthroline (BPhen) as electron transporting layer (ETL) and hole blocking layer (HBL)/Liq as electron injection layer (EIL)/Al as cathode, where the doping con-centrations of FIrpic in mCP and TPBi were optimized at 8 wt.%, respectively. Device A had FIrpic doped in mCP of 8 wt.% (30 nm) single emitting layer. Device B had FIrpic doped in mCP of 8 wt.% (15 nm) and FIrpic doped in TPBi of 8wt.%

(a)

FIrpic   TPBi   mCP

(b)
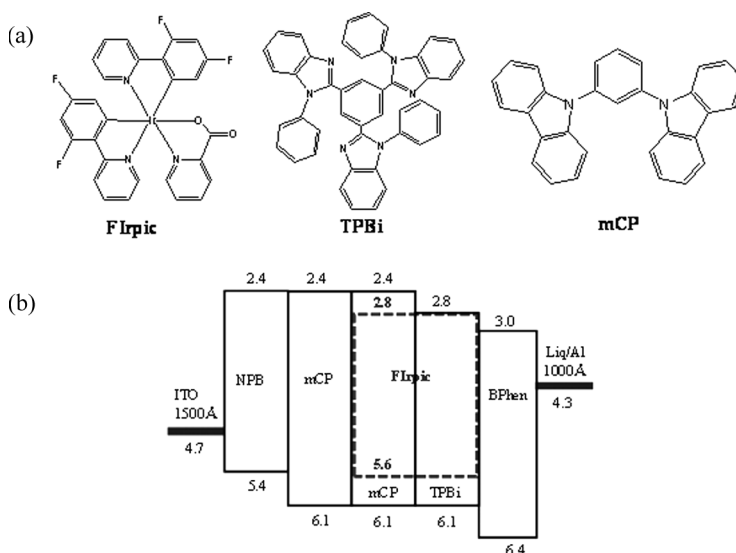
Figure 1. (a) Molecular structure of the key materials used for fabrication. (b) The energy level diagram of device A and B. Numbers indicate the highest occupied molecular orbital and lowest unoccupied molecular orbital of various materials used in this study.

(15 nm) as D-EML layers. XBL are inserted between HTL and BEML-1 for efficient exciton confinement [9,14] Device A with single EML have exciton formation zone (EFZ) at mCP side at the interface of mCP and BPhen. On the other hands, device B with D-EML is expected to have EFZ both at mCP and TPBi side at the interface of mCP and TPBi. Moreover, mCP and TPBi are a well-known hole-transport – type, and electron transport – type material, respectively. Therefore, holes are accumulated at the interface of mCP and TPBi layer.

Figure 2 shows the current density versus voltage characteristics and inset Figure 2 shows luminance versus voltage characteristics of blue PHOLEDs with different EMLs. Device A and B showed the maximum current density of 34.1 and 77.6 mA/cm^2 at 10 V, respectively. Device B showed the highest current density at the whole driving voltages. This indicates that device B had a much smaller electron-injection barrier of nearly 0.2 eV between lowest unoccupied molecular orbital (LUMO) of the BPhen and LUMO of TPBi than that (0.6 eV) of device A (BPhen-mCP) as shown in Figure 1. All devices showed the maximum luminance of 2580 and 4530 cd/m^2 at 10 V, respectively, where device B showed higher luminance than device A. Typically, phosphorescent blue OLED exhibits a higher driving voltage due to the wide band gap of the host material. In our TPBi-based OLED, besides the high electron mobility of TPBi which provides a good transport characteristics, barrier height of hole injection from mCP to TPBi is not exist because the HOMO values of mCP and TPBi are same, which results in a low driving voltage in TPBi-based devices.
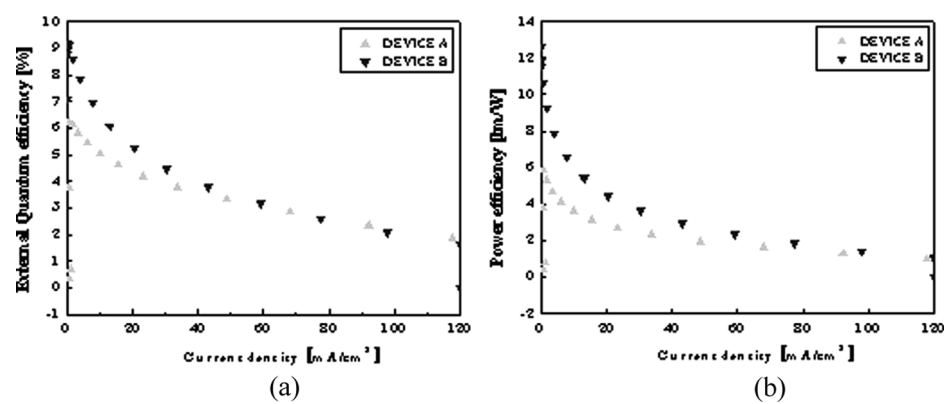
The EQE and power efficiency versus current density characteristics of the blue PHOLEDs were showed in Figure 3(a) and (b). Device A and B showed the maximum EQE of 6.24 and 5.85% at 0.903 and 0.205 mA/cm^2 and maximum power
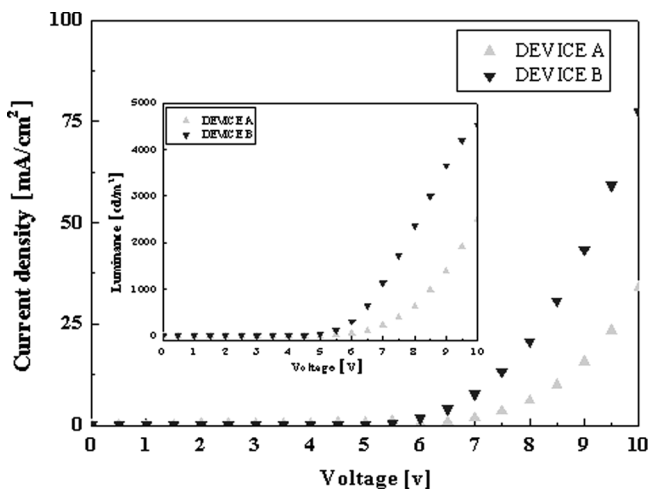
Figure 2. Current density versus voltage characteristics of device A and C at 10 V. Inset: Luminance versus voltage characteristics of device A, B and C at 10 V.

efficiency of 5.85 and 12.62 lm/W at 0.903 and 0.051 mA/cm^2, respectively. Device B exhibited higher EQE than device A, which seems to be due to D-EML structure. Since the triplet energy of mCP (2.9 eV) and TPBi (2.8 eV) is higher than that of FIrpic (2.65 eV), the triplet confinement of FIrpic between mCP and TPBi is expected [10,11]. In addition, the HOMO level of TPBi (6.1 eV) is similar to mCP (6.1 eV). It was also found that the device B exhibits higher efficiency than device A, which seems to be due to proper balance of holes and electrons transported into D-EML by using same thickness of mCP layer in device B, where the hole mobility of mCP is similar to electron mobility of TPBi.

Figure 4(a) shows the CIE$_{x,y}$ coordinate of the devices A and B. The device A and B showed CIE$_{x,y}$ coordinates (x = 0.17, y = 0.34) and (x = 0.17, y = 0.35) at 1000 cd/m^2, respectively. All devices shows similar color chromaticity. Figure 4(b)

Figure 3. (a) External quantum efficiency versus current density characteristics of device A and B. (b) Power efficiency versus current density characteristics of device A and B.
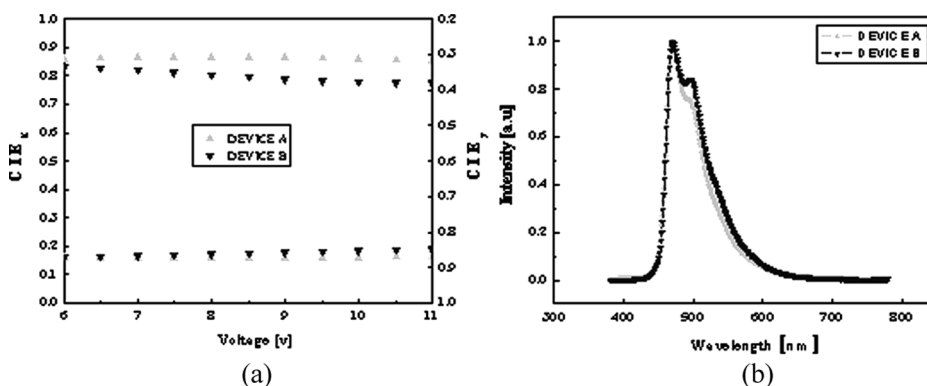
Figure 4. (a) Commission Internationale de I'Eclairage coordinates versus voltage characteristics of device A and B. (b) electroluminescence spectra for device A and B.

also shows EL spectra of the all devices at 10 V, where device A and B had same maximum peak at 471 nm due to the emission from FIrpic.

Conclusions

In this paper, we demonstrated lower driving voltage and efficient blue PHOLEDs by using iridium FIrpic doped in D-EML, mCP and TPBi. The triplet energy of mCP and TPBi is higher than that of FIrpic. Therefore D-EML exhibited efficient exciton confinement and broad exciton formation zone. The optimized blue PHOLEDs of D-EML of mCP:TPBi(1:1) exhibited a peak external quantum efficiency (EQE) of 9.22% at 0.21 mA/cm^2, power efficiency of 12.62 lm/W at 0.05 mA/cm^2, current efficiency of 18.89 cd/A at 0.21 mA/cm^2, and CIE$_{x,y}$ coordinates of (0.17, 0.35) at 1000 cd/m^2, respectively.

Acknowledgments

References

[1] Tang, C. W., & Van Slyke, S. A. (1987). *Appl. Phys. Lett.*, *51*, 913.
[2] Baldo, M. A., Thompson, M. E., & Forrest, S. R. (2000). *Nature*, *403*, 750.
[3] Kido, J., Hongawa, K., Okuyama, K., & Nagai, K. (1994). *Appl. Phys. Lett.*, *64*, 815.
[4] D'Andrade, B. W., Holmes, R. J., & Forrest, S. R. (2004). *Adv. Mater.*, *16*, 624.
[5] D'Andrade, B. W., & Forrest, S. R. (2005). *Adv. Mater.*, *16*, 1585.
[6] Pfeiffer, M., Forrest, S. R., Leo, K., & Thompson, M. E. (2002). *Adv. Mater.*, (Weinheim. Ger.) *14*, 1633.
[7] Watanabe, S., Ide, N., & Kido, J. (2007). *Jpn. J. Appl. Phys.*, Part 1 *46*, 1186.
[8] Kim, S. H., Jang, J., & Lee, Y. (2007). *Appl. Phys. Lett.*, *90*, 223505.
[9] Fukagawa, H., Watanabe, K., Tsuzuki, T., & Tokito1, S. (2008). *Appl. Phys. Lett.*, *93*, 133312.

[10] Yook, K. S., Jeon, S. O., Joo, C. W., & Lee, J. Y. (2008). *Appl. Phys. Lett.*, *93*, 113301.

[11] Jonghee Lee, Jeong-Ik Lee, & Hye Yong Shu (2009). *Synthetic Metals.*, *159*, 1460.

[12] Tokito, S., Iijima, T., Tsuzuki, T., & Sato, F. (2003). *Appl. Phys. Lett.*, *83*, 2459.

[13] Tokito, S., Iijima, T., Tsuzuki, T., & Sato, F. (2003). *Appl. Phys. Lett.*, *83*, 2459.

[14] Gufeng He, Martin Pfeiffer, Karl Leo, Michael Hofmann, Jan Birnstock, Robert Pudzich, & Josef Salbeck (2004). *Appl. Phys. Lett.*, *85*, 3911.